Pharm Res (2012) 29:3464–3474
DOI 10.1007/s11095-012-0841-2

RESEARCH PAPER

Assessment of Iontophoretic and Passive Ungual Penetration by Laser Scanning Confocal Microscopy

Julie Dutet • M. Begoña Delgado-Charro

Received: 31 May 2012 / Accepted: 13 July 2012 / Published online: 7 August 2012

ABSTRACT

Purpose To estimate the *in vitro* ungual penetration depth of sodium fluorescein and nile blue chloride by laser scanning confocal microscopy.

Methods The depth, uniformity and pathways of penetration of both markers into human nail during passive and iontophoretic experiments were investigated. The penetration of sodium fluorescein into the dorsal, ventral and intermediate layers of the nail was also studied. Transversal images were used to estimate directly the relative penetration of the markers with respect to the complete thickness of the nail. "Exposed layer" images allowed estimating the depth of penetration by taking xy-plans, starting by the exposed layer, and following the z axis into the nail.

Results The fluorescent markers penetrated 7–12% of the nail thickness. Iontophoresis increased penetration of both markers compared to passive diffusion. However, ungual penetration was not modified by the intensity of current applied. Penetration into the dorsal, ventral, and intermediate nail layers was similar. The method developed allowed inter- and intra- nail variability to be accounted for.

Conclusions Iontophoresis enhanced moderately the penetration of the two markers into the nail plate as compared to passive diffusion. The confocal images suggested the transcellular pathway to be predominant during both passive and iontophoretic experiments.

J. Dutet • M. B. Delgado-Charro (✉)
Department of Pharmacy and Pharmacology, University of Bath
Claverton Down
Bath BA2 7AY, UK
e-mail: B.Delgado-Charro@bath.ac.uk

Present Address:
J. Dutet
ICTA PM
11 rue du Bocage
21121 Fontaine-lès-Dijon, France

KEY WORDS depth · iontophoresis · nail · pathways · laser scanning confocal microscopy

ABBREVIATIONS

LSCM	laser scanning confocal microscopy
NBC	nile blue chloride
SF	sodium fluorescein

INTRODUCTION

In the last 15 years there has been a renewed interest in the area of nail drug delivery (1–3). Systemic treatments are commonly used for onychomycosis and nail psoriasis and, while effective, they can result in undesirable side effects and drug interactions (4–7). Topical therapies circumvent these problems but have limited efficacy (4,8). Thus, there is a need to develop more efficient topical methods to treat nail disease and an important amount of work has addressed different methods to enhance nail penetration as recently revised (1–3).

Iontophoresis enhances molecular transport across a biological membrane via the application of low intensity electrical currents and is being considered as a method with which to improve drug delivery to the nail. The applications of iontophoresis in nail drug delivery have been recently reviewed (9). Briefly: two mechanisms, electro-repulsion and electro-osmosis drive molecules into and through the nail according to their polarity and the nail plate permselectivity. Electro-transport of small ions is governed by similar rules to those regulating transdermal iontophoresis, that is; molar fraction and mobility are the key determinants of transport numbers during nail iontophoresis. On the other hand, while there is evidence for nail permselectivity, the convective transport across the nail seems a relatively variable and not very efficient phenomenon. *In vivo* nail iontophoresis has

been successfully implemented (10,11) and the data gathered so far seem to support the practical use of the technique. In the case of transdermal iontophoresis, molecular transport occurs through both the appendegeal and intercellular pathways (12,13). In the case of the nail, only the transcellular and paracellular pathways are available for transungual permeation. However, the pathways of drug permeation into the nail plate have not been directly elucidated.

The human nail plate consists of many layers of compacted keratinized cells (14). The highly organized structure of the keratins and the thickness of the plate explain the poor penetration which most actives have across the nail. For example, a study by De Berker (15) found the thickness of toenail plates to vary between 500–1240 μm and the number of cells in the dorso-ventral axis to range from 134 to 226. The nail plate is produced primarily (80%) by the nail matrix; the ventral aspect of the proximal nail fold may contribute to part of the dorsal nail plate whereas the contribution of the nail bed to the ventral nail plate remains a controversial issue (14,15). Regardless of this debate, the nail plate is not homogenous and has been divided in either two or three layers depending on the criteria used (14,16–19). The dorsal, intermediate and ventral layers differ in their chemical composition, ultrastructure and keratin fibres orientation (14,16–19). According to Kobayashi *et al.* (16) the permeability of drugs also differs across these three layers, and assuming a 3:5:2 thickness ratio for the dorsal:intermediate:ventral layers the authors concluded the dorsal layer to be the main barrier to drug permeation. On the other hand, recent work (20) investigated the microstructure of nails via mercury intrusion porosimetry. According to the authors, the nail could be modelled as a banded structure having an inner, less porous region and two outer regions with higher porosity.

Laser Scanning Confocal Microscopy (LSCM) has been used to visualise the skin structure and penetration pathways of fluorescent markers into the skin during passive and iontophoretic transport (12,21). In contrast, LSCM of human nails has mostly investigated the nail structure and the diagnosis of onychomycosis (22–24). Light microscopy was used by Nair *et al.* (25) to investigate nail penetration of methylene blue under iontophoretic and passive conditions. The dye intensity was greater when iontophoresis was used but the technique did not allow for pathway identification. Thus, to the best of our knowledge, this is the first time that LSCM is used to specifically investigate the depth, uniformity and pathway of penetration of compounds into the human nail under iontophoretic and passive conditions.

In this work, the passive and iontophoretic penetration of sodium fluorescein (SF), a hydrophilic anionic compound (376.28 Da, log$P$=−0.67) and of nile blue chloride (NBC), a lipophilic cationic compound (353.85 Da, log$P$=4.99) into human nail was investigated. A first objective aimed to investigate whether the depth of penetration, as determined via LSCM, was modified by current application or by exposing different (dorsal, ventral and intermediate) layers of the nail to the donor solution. A second objective aimed to compare three different methods of estimating depth of penetration based on LSCM imaging and to establish their possible use as quantitative tools. For this, an estimation of the inter- and intra- nail variability in the depth of penetration determined by the three methods was done.

MATERIALS AND METHODS

Materials

Sodium fluorescein (SF), nile blue chloride (NBC) and sodium chloride were obtained from Sigma Aldrich Co. (Gillingham, UK). Silver wire, silver chloride powder and platinum wire were used to prepare the electrodes, had a minimum purity of 99.99% and were obtained from Sigma Aldrich Co. (Gillingham, UK). All aqueous solutions were prepared using high purity deionised water (18.2 MΩ.cm, Barnstead Nanopure Diamond™, Dubuque, IA, USA).

Human Nails

Ethical approval was granted by the Bath Local IRB and finger nail clippings were obtained from fourteen healthy volunteers who gave their written informed consent. The harvested nails were washed with deionised water and kept at room temperature in desiccators until use. Prior to each experiment, the nail's thickness was measured with a point micrometer (Point Anvil Micrometer, Mitutoyo, Andover, UK) on the portion of the nail which was the closest to the hyponychium.

Some nails were filed to expose the intermediate layer. In this case, the initial thickness was measured at the centre of the nail and the dorsal layer of the nail was manually filed off using a manicure metallic file until ~30% of the initial thickness was removed.

Experimental Set Up

A minimum of three independent replicates (one nail per cell, one cell at a time) of each condition were performed at room temperature. Experiments were performed in Franz vertical diffusion cells (PermeGear Inc., Bethlehem, PA, USA) presenting a transport area of 0.20 cm^2. Each nail was soaked in deionised water during 10–15 min prior to the experiments in order to recover some flexibility (9), and then placed in a 5 mm (0.20 cm^2 transport area) nail adapter (PermeGear Inc., Bethlehem, PA, USA). The

ensemble was placed between the two chambers of Franz vertical diffusion cells (PermeGear Inc., Bethlehem, PA, USA).

The bottom chamber (3.2–3.6 ml) was used to hold the donor solution while the top chamber was used to hold the receptor solution (0.7 ml). The nail adapter was orientated accordingly to the layer which was exposed to the donor chamber. All experiments lasted 18 h during which sink conditions were maintained.

In the case of iontophoretic experiments, constant direct current was applied using a power supply (Kepco APH 1000 M, Flushing, NY) via homemade Ag/AgCl electrodes (26). Preliminary tests showed the initial voltage required to pass 0.1 and 0.4 mA through some nails at initial times was relatively high so the power supplier was set with a maximum voltage output of 200 V. Thus, the actual current passed through the nails with the highest electrical resistance was less than the nominal 0.1 or 0.4 mA during the first 30 min of the experiment. The voltage was monitored during the first two hours of each experiment.

Nile Blue Chloride Experiments

Passive, 0.1 and 0.4 mA iontophoresis experiments (NBC-Passive, NBC-0.1 and NBC-0.4 respectively) were performed on intact nail clippings with the donor chamber facing the dorsal layer. The donor solution contained 1%w/v (28 mM) NBC and 50 mM NaCl which provided sufficient chloride ions for the anodal reaction. The pH of the donor solution was ~3 which allowed NBC to be totally ionised (pKa ~9.5). The donor was replaced at 4 h. The 0.7 ml receptor solution consisted of 0.9% (154 mM) NaCl.

Sodium Fluorescein Experiments

Passive, 0.1 and 0.4 mA iontophoresis experiments (SF-Passive, SF-0.1 and SF.0-4 respectively) were performed with the 375 mM SF donor solution facing the dorsal layer. The pH of the donor solution was ~8. Therefore SF (pK_{a1} ~4.5 and pK_{a2} ~6.5) was predominantly (97%) in its di-anionic form. The donor was replaced at 4 h. The 0.7 ml receptor solution contained 154 mM and 1.37 M of NaCl for the 0.1 and 0.4 mA experiments respectively, to provide sufficient chloride ions for the electrode electrochemical reaction.

One passive (SF.V-Passive) and one 0.1 mA iontophoretic (SF.V-0.1) experiment exposed the ventral layer of the nail to the donor solution (375 mM SF). One 0.1 mA iontophoretic experiment (SF.I-0.1) exposed the intermediate layer to the donor solution (375 mM SF). In these three experiments, the receptor was 154 mM NaCl and the donor was replaced at 4 h.

Sample Preparation

At the end of the experiment, the nail adapter was taken out of the cell and the exposed area of the nail was washed under a thin dribble of running deionised water and patted dry before separating the nail from the adapter. Then, the nail was washed in three successive baths containing deionised water and patted dry between each bath. Finally, the nail was cut with a scalpel. The cuts were performed in the receptor-to-donor direction to minimize contamination. A minimum of four polygonal pieces (used for "exposed layer" images) and four thin slices (for "transversal images") were obtained from each nail (Fig. 1).

LSCM Analysis

All the observations were performed on a LSM Meta 510 microscope (Zeiss, Oberkochen, Germany) and the images were treated using a Zeiss LSM image browser version 4.0.0.157. Nails exposed to NBC donor solutions were analysed using a helium neon laser (λ_{ex}=633 nm) with dichroic beam splitter HFT 488/543/633, a LP 650 and a NFT 490 filters. Nails exposed to SF donors were analysed using an argon laser (λ_{ex}=488 nm), a NFT 545 and a LP 505 filter.

"Exposed layer" images taken with an ×10 objective were made on a black background and used to estimate the penetration depth. In this case, x-y planar images were taken every 2 µm NBC and 5 µm for SF and used to build a three dimensional image. Additional "exposed layer" images were taken at ×20 objective under halogen light to investigate the pathways of penetration of the fluorescent markers into the nails. In this case, x-y images were taken every 1 µm (SF) or 2 µm (NBC).

All transversal images were taken at ×10 objective and under halogen light. The xy-plans were taken below

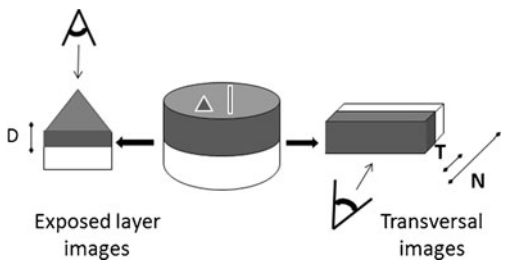

Fig. 1 Schematic representation of the mechanical cuts performed to prepare nail samples for confocal microscopy analysis. The grey area represents the side of the nail in contact with the donor solution through which the marker has penetrated. Left: exposed layer images, x-y planar images were taken every 2 μm NBC and 5 μm for SF and used to build a three dimensional image. The permeation depth "D" was measured as the thickness of the fluorescent band in the 3 D reconstruction. Right: Transversal images allowed measuring directly the depth of penetration "T" and the total nail thickness "N". The parameter T% was calculated as (T*100/N).

the surface to avoid possible artefacts caused by the mechanical cut.

As a control, 3 nails which have been soaked in 154 mM NaCl for 18 h were examined by LSCM. This control showed that the intensity of the laser used was too low cause interferences due to auto-fluorescence of the nail.

Data Analysis and Statistics

Three measurements of marker penetration: D, T and %T, were obtained for each nail and experiment. In the case of the "exposed layer" images, successive images (*xy*-plans) were taken at different depths starting from the surface of the layer exposed to the donor to the deeper areas of the nail (following the *z* axis). All the images obtained were then used to reconstruct a three dimensional image of the fluorescent marker penetration. The measured depth of penetration using these images is referred to as "D".

The thin slices used for transversal imaging allowed visualisation of the markers penetration (T) simultaneously with the whole nail thickness (N). This allowed estimation of the fluorescent marker absolute penetration "T" as well as its relative penetration (%T) (percentage of marker penetration relative to the entire nail thickness on the same image or %T=Tx100/N).

All data are presented as mean±SD unless otherwise indicated. Data analysis was performed with Graph Pad Prism version 5.00 (Graph Pad Software, San Diego California USA). Voltage values were compared using a two-way ANOVA followed by a Dunns' post-test. Linear regression was used to investigate whether thickness of the nail had an effect on the voltages observed during iontophoresis. A non-parametric Kruskal-Wallis followed by a Dunns' post-test was used to compare the depth of penetration expressed as D, T and %T measured under different treatments (passive, 0.1 and 0.4 mA) and different nails. When comparing treatments the analysis used all the measurements taken for all the nails used in the respective condition. When only two sets of data were compared, a non-parametric unpaired Mann Whitney t-test was performed. The level for statistical significance was set to $p<0.05$.

RESULTS

LSCM examination of nails after passive and iontophoretic transport experiments was done to determine how deeply the two fluorescent markers penetrated the nail plate. The possible effect of current intensity and nail layer (dorsal, intermediate, ventral) on the markers penetration was also investigated. The inter- and intra- nail variability associated to the measurements of depth was examined and the results obtained using three different parameters (D, T, %T) were compared.

Figure 2 shows that voltage decreased rapidly upon current application. Lower values were observed during the experiments performed with filed nails, probably due to their reduced thickness, but the differences were not significant. Overall, the current application time was the most significant factor as indicated by a two-way Anova. A relation between nail thickness and voltage was only found for the 30 min-voltage measured in the 0.1 mA experiments ($r^2=0.67$). Typically, the voltages measured during *in vitro* nail iontophoresis are higher than those measured during *in vivo* nail iontophoresis as shown by Dutet (11) and Hao (27). Therefore, the values here reported cannot be extrapolated to the *in vivo* situation.

NBC experiments used nail clippings donated by six female participants (21–52 years) with a thickness 287±31 μm ($n=3$); 300±78 μm ($n=3$) and 287±38 μm ($n=3$) for the NBC-Passive; NBC-0.1 and NBC-0.4 experiments, respectively. NBC penetration into the nail plate after 18 h was estimated via LSCM and expressed as D, T, and %T. Figure 3 shows representative images for the NBC-Passive, NBC-0.1 and NBC-0.4 experiments as well as the average D, T and T% measured for each nail. Because the depth penetration was measured in several replicates for each nail it was possible to evaluate inter-nail variability. The average D values increased with current application (Table I) but the differences were not statistically significant. On the other hand, the T and %T parameters were significantly higher ($p<0.05$) for the iontophoretic experiments although increasing the current applied to 0.4 mA had no significant effect.

SF experiments used nail clippings donated by 4 female participants (21–44 years) with a thickness 237±25 μm ($n=3$); 265±47 μm ($n=4$) and 246±21 μm ($n=3$) for the SF-Passive; SF-0.1 and SF-0.4 experiments, respectively. After 18 h of experiment, the nail samples were analysed by LSCM and the depth of penetration estimated as D, T and T%. Figure 4 shows representative images for the SF-Passive, SF-0.1 and SF-0.4 experiments. The D, T and T%

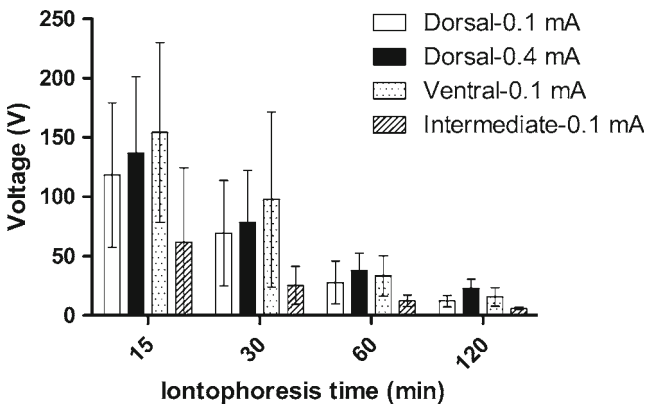

Fig. 2 Voltage measured between the cathode and anode of each iontophoretic cell for the different iontophoretic conditions tested and as a function of time. Values are mean±SD of $n=3–7$.

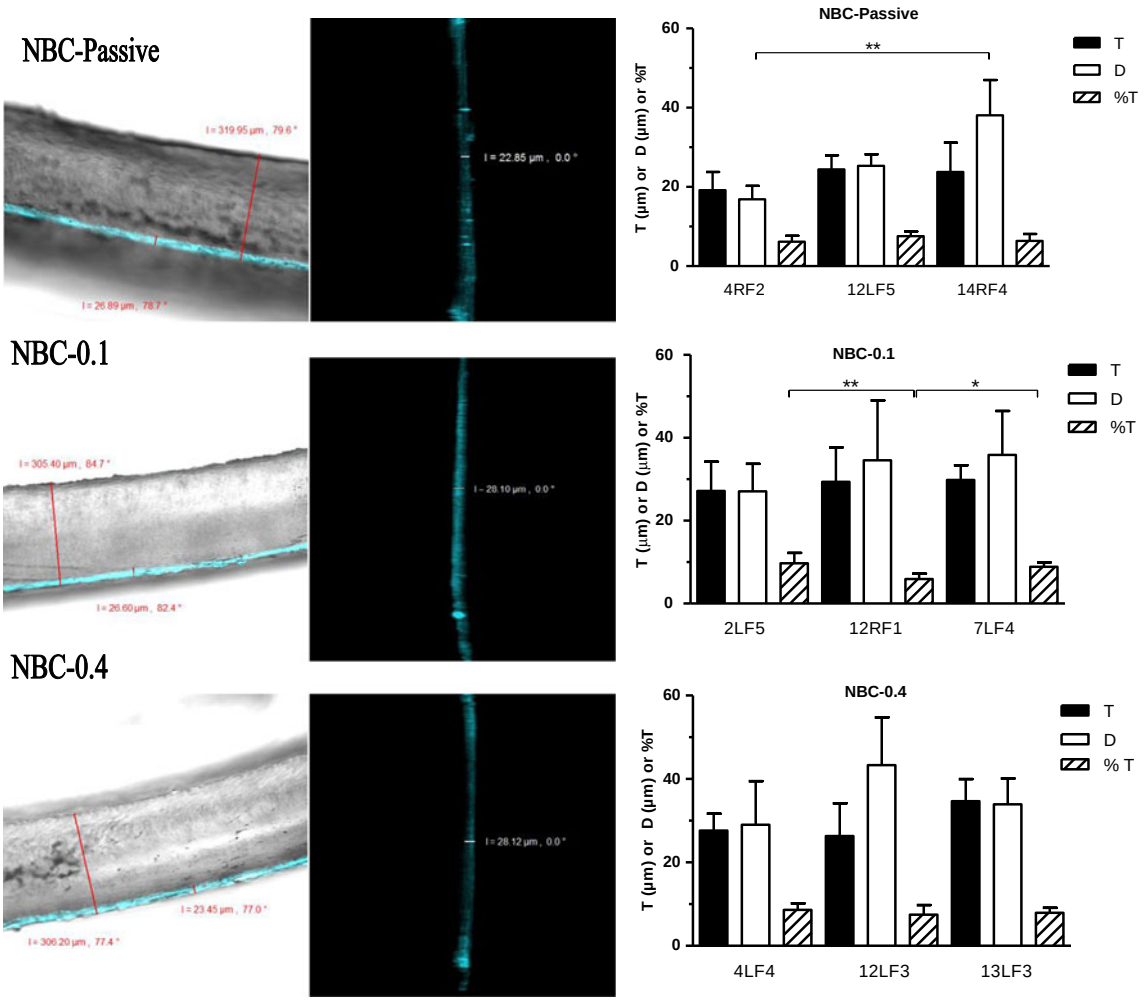

Fig. 3 Left panel: Representative confocal images of transversal cuts allowing direct measurement of NBC penetration depth T (shorter red line) and %T (Tx100/N). The longer red line indicates the thickness of the nail "N". Central panel: Representative 3-D reconstruction of *xy*-planar images of "exposed layer" images obtained at different depths, the exposed dorsal layer faces the right for NBC-Passive and NBC-0.4 experiments and faces the left for the NBC-0.1 experiment. The white line indicates the depth of penetration "D". Right panel: NBC depth of penetration (expressed as T, D and %T) measured for each nail (Mean±SD; n=5–8 images). The symbols * and ** indicate significant ($p<0.01$–0.05) and very significant ($p<0.001$–0.01) differences between pairs of bars. The first digit in the nail code indicates the participant number, L or R indicate left or right hand and F+ digit indicates the finger where F1 = thumb.

values for each nail and the average for each treatment are shown in Fig. 4 and Table I, respectively. In this case, the three parameters indicated that iontophoresis increased significantly ($p<0.05$) the depth of SF penetration into the nail plate. Again, the effect of current intensity did not reach statistical significance.

One passive (SF.V-Passive) and one 0.1 mA iontophoretic (SF.V-0.1) experiment which exposed the ventral layer to the donor solution were also performed. These experiments used nails from five different female donors (21–28 years) having a 353±29 µm (n=3) and 242±33 µm (n=4) average thickness for the SF.V-Passive and SF.V-0.1 experiments, respectively. A final experiment SF.I-0.1 used filed nails which aimed to expose the intermediate layer of the nail to the donor solution. Three replicates used nails from 3 female donors (22 and 44 years) the thickness of which had been reduced from 277±49 µm to 200±46 µm. The results from these three experiments are summarized in Fig. 5 and Table I. Iontophoresis significantly ($p<0.05$) delivered SF deeper than passive diffusion into the ventral layer of the nail as indicated by D, T and %T. SF penetrated more deeply into the dorsal and intermediate layer (Table I) than into the ventral layer. However, these last observations were indicated only by D measurements.

The depth of penetration of SF and NBC into the dorsal layer was also compared. Analysis of transversal view images (T), tend to indicate that SF penetrated significantly deeper than NBC during iontophoresis and passive experiments. However, analysis of the "exposed layer" images (D) found no differences in the iontophoretic experiments and, in

Table I NBC and SF Penetration Depth Into the Nail Plate as Reported by T, %T and D after 18 h of Iontophoretic or Passive Delivery. All Values are Given as Mean±SD of 15–27 Measurements (n) Taken on 3–4 Nails

Experiment	T (μm)	n[a]	D (μm)	n[a]	%T	n[a]
NBC-Passive	22±5	19	25±11	17	6.7±1.6	19
NBC-0.1	28±6[b]	20	33±11	16	8.3±2.3[b]	27
NBC-0.4	30±7[b]	20	34±9	19	8.0±1.6[b]	20
SF-Passive	26±4[g]	17	19±4[g]	15	7.8±1.5	17
SF-0.1	34±7[c,g]	27	34±9[c]	25	9.4±2.2[c]	27
SF-0.4	39±8[c,g]	21	37±6[c]	19	11.3±2.6[c,g]	21
SF.V-Passive	26±5	18	15±4[c]	15	7.5±2.0	18
SF.V-0.1	31±7[d]	27	21±3[d,e,f]	24	9.3±2.3[d]	27
SF.I-0.1	30±6	18	30±6	19	11.2±2.7	18

[a] n, number of measurements performed

[b] Significantly different to NBC-Passive

[c] Significantly different to SF-Passive.

[d] Significantly different to SF.V-Passive

[e] Significantly different to SF-0.1.

[f] Significantly different to SF.I-0.1

[g] Significantly different depths measured for NBC and SF for equivalent experiments.

contradiction with T images, a deeper passive penetration of NBC. When %T was considered, SF went significantly deeper than NBC only during 0.4 mA iontophoretic experiments. On the whole the most consistent finding was that SF penetrated deeper than NBC into the nail plate during 0.4 mA iontophoresis experiments.

An attempt was made to elucidate the pathways of penetration of the two fluorescent markers, by taking images at an objective ×20. Figure 6 shows representative images obtained. No images are shown for SF-Passive, SF.V-Passive because of their poor resolution. No striking differences were observed between the images of passive and iontophoretic permeation of NBC. As a general rule, the fluorescence was quite spread over the nail surface suggesting the marker followed the transcellular pathway. In some zones the intercellular pathway seemed slightly darker demarcating the cells. In the case of SF, the images also supported that the marker followed a transcellular pathway during iontophoresis independently of the layer (dorsal, ventral, and intermediate) exposed to the donor solution. In addition, it was possible to notice some dark regular intracellular spots (indicated by white arrows) in the SF images, which did not exist in the NBC images.

DISCUSSION

This work investigated the possible use of LSCM as a tool with which to assess molecular penetration into the nail plate by iontophoretic and passive means. To do this, the depth of penetration was expressed via three parameters derived from LSCM imaging of transversal and exposed images of the nail. An important component of this assessment was to quantify both the inter- and intra- nail variability observed in the measurement of depth taken. To assess the degree of intra-nail variability, that is, how much the depth of penetration varied for different parts of the same nail, a minimum 4 thin and 4 polygonal samples were cut from each nail. In this way, the coefficients of variation (CV%) for the T, D and %T values estimated for each nail were determined. The average CV% associated with the T, D and %T values in the NBC-Passive, NBC-0.1 and NBC-0.4 experiments were 21.7±7.6; 26.0±9.2 and 21.0±6.4. The average CV% for the T, D and %T values and the SF-Passive, SF-0.1 and SF-0.4 experiments were 19.5±4.5; 16.0±3.4 and 18.8±5.7. However, the coefficient of variation (CV%) for individual nails ranged from 12 to 31%, from 9 to 42% and from 11 to 30% for the T, D and %T values. Several nails were examined for each condition to assess inter-nail variability. The results in Figs. 3, 4 and 5 show that there were significant differences ($p<0.05$) in the penetration depth measured for nails submitted to the same protocol (NBC-Passive, NBC-0.1; SF-Passive, SF-0.1, SFV-Passive, SF.V-0.1 and SF.I-0.1). These results suggest that assessment of penetration by LSCM should be based in multiple images and be accompanied by some measurement of the inter- and intra- variability associated to the parameter used to express the depth. In absence of this information, the quantitative comparison of the penetration depth and consequently, the objective discrimination between formulations or treatments, is problematic.

The results in Table I suggest that T measurements performed slightly better than D measurements in detecting differences, for example in NBC experiments. This could be explained by the lower CV% for the T values in this case. Another consideration is that D measurements are reconstructions of xy planar images taken every 2 (NBC) or 5 (SF) μm and this distance should be taken into account to interpret data. In contrast, T and %T values are directly read from the image and, because they are taken on transversal cuts, their resolution is not altered for the deeper layers of the nail. As discussed above (Table I) the three parameters used did not always agree whether differences in penetration depth existed or not. Thus, the complementary assessment of T, D and %T seems a more robust method to determine and compare depth of penetration.

In the case of passive experiments little differences were found between the two markers. This is expected as SF and NBC have similar molecular weight, a parameter identified as the key determinant of the nail permeability coefficient (28–30). The two markers primarily differ in their lipophilicity and it was shown that logP either decreased or did not

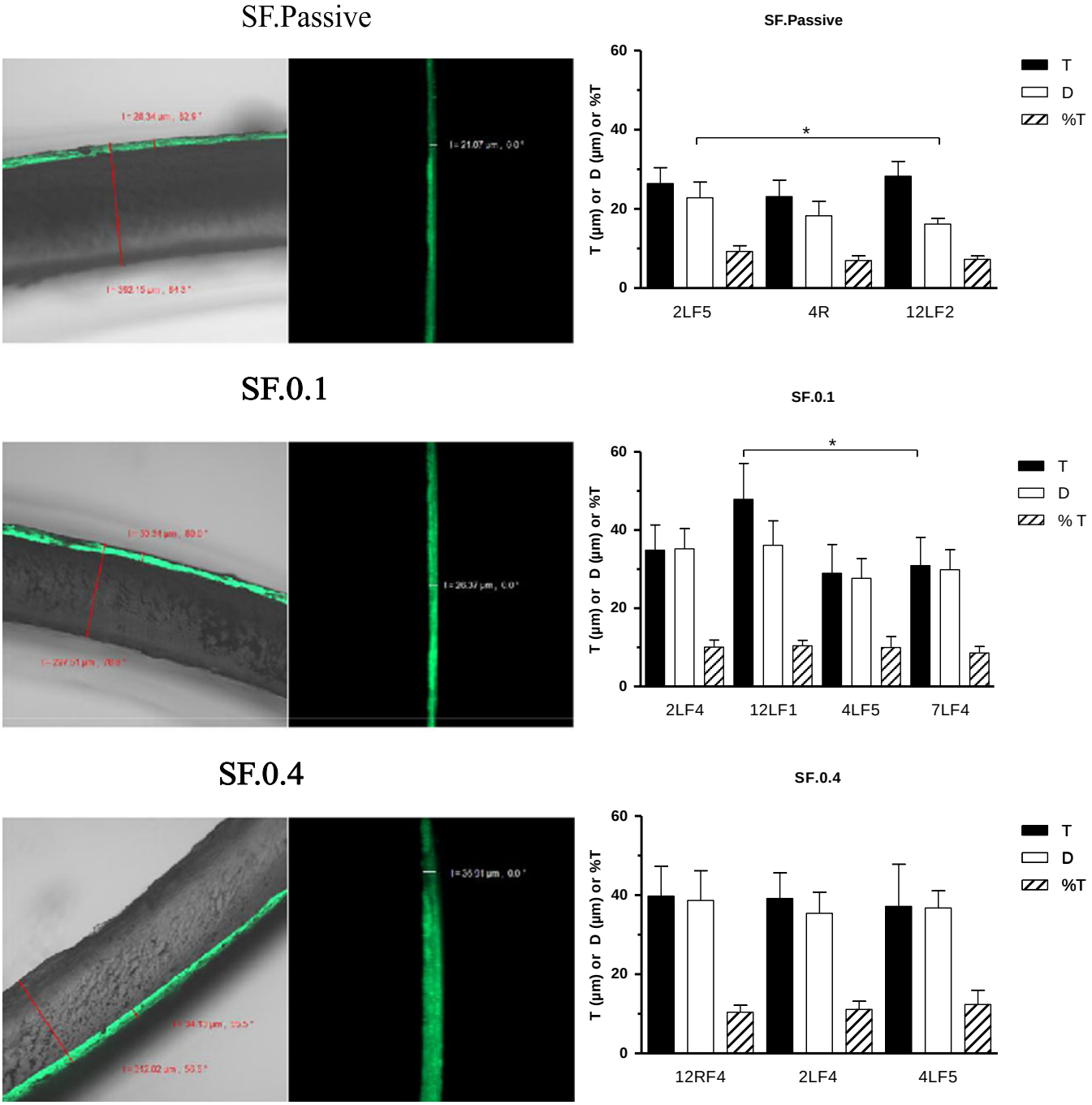

Fig. 4 Left panel: Representative confocal images of transversal cuts allowing direct measurement of SF penetration depth T (shorter red line) and %T (Tx100/N). The longer red line indicates the thickness of the nail "N". Central panel: Representative 3-D reconstructions of *xy*-planar images of "exposed layer" images obtained at different depths, the exposed dorsal nail layer faces the right of the image. The white line indicates the depth of penetration "D". Right panel: SF depth of penetration (expressed as T, D and %T) measured for each nail (Mean±SD; n=5–8 images). The symbols * and ** indicate significant ($p<0.01$–0.05) and very significant ($p<0.001$–0.01) differences between pairs of bars. The first digit in the nail code indicates the participant number, L or R indicate left or right hand and F+ digit indicates the finger where F1 = thumb.

modify the permeability coefficient of permeants across the nail (28–30). It could also be argued that the depth of penetration at a given time is closely related to the diffusional lag time, and therefore primarily determined by the diffusivity, i.e., molecular weight. Finally, the poor penetration observed after 18 h is consistent with previous work which could not measure transport across the nail plate for compounds with molecular higher than 250 Da (30) and reported a lower nail permeability for ionized compounds (29,30).

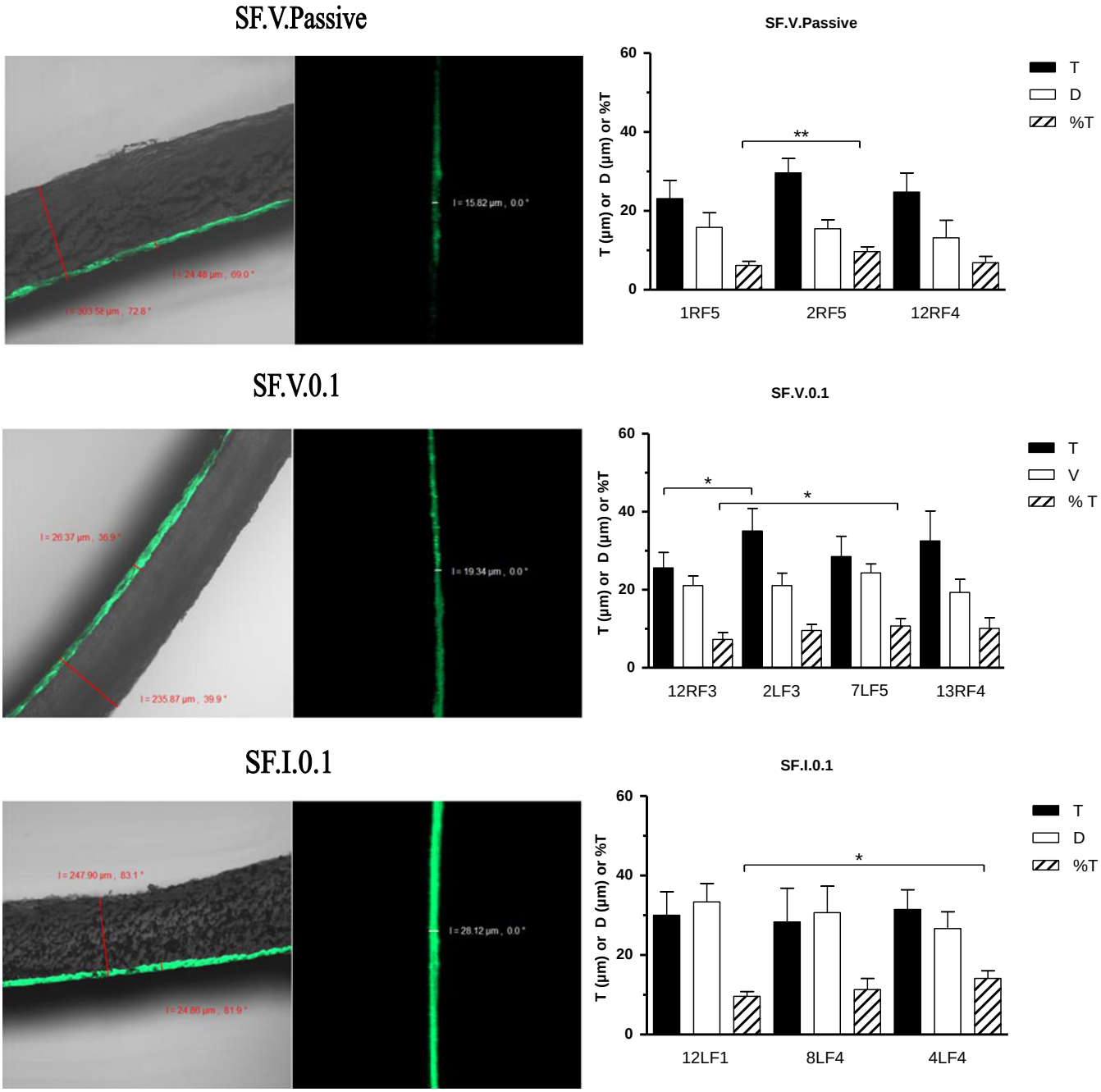

Fig. 5 Representative confocal images illustrating SF penetration: passively into the ventral layer (SF.V-Passive) and iontophoretically into the ventral (SF.V-0.1) and intermediate layer (SF.I-0.1). Left panel shows transversal cuts allowing direct measurement of the marker penetration depth T (shorter red line) and %T (Tx100/N). The longer red line indicates the thickness of the nail "N". Central panel shows 3-D reconstructions of *xy*-planar images of "exposed layer" images obtained at different depths, the nail surface in contact with the donor solution (ventral layer in this case) faces the left of the image. The white line indicates the depth of penetration "D". Right panel: SF depth of penetration (expressed as T, D and %T) measured for each nail (Mean±SD; n=5–8 images). The symbols * and ** indicate significant ($p < 0.01$–0.05) and very significant ($p < 0.001$–0.01) differences between pairs of bars. The first digit in the nail code indicates the participant number, L or R indicate left or right hand and F+ digit indicates the finger where F1 = thumb.

Overall, iontophoresis enhanced nail penetration of the two fluorescent markers as compared to passive diffusion. However, the differences observed between passive and iontophoretic depth of penetration were relatively modest. Further, increasing the intensity of the current applied from 0.1 to 0.4 mA had no significant effects on the markers penetration. Likewise, greater differences were expected among the iontophoretic penetration of the two markers. While the parameters T (0.1 and 0.4 mA experiments) and T% (0.4 mA) were significantly different for NF and NBC

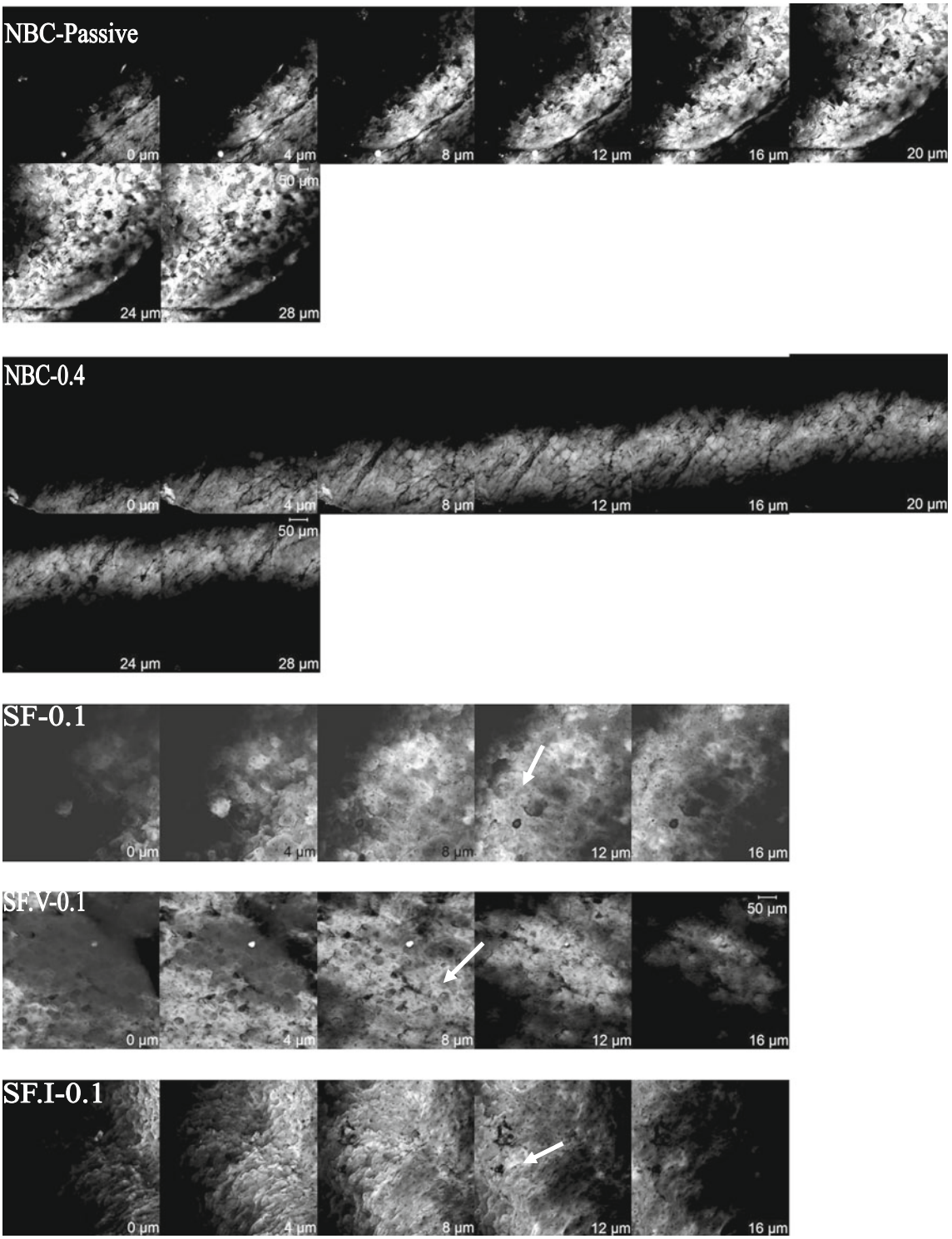

Fig. 6 Visualisation of NBC and SF pathway of penetration into the nail. Both fluorescent markers are shown in white to facilitate comparison. White arrows indicate darker areas on SF images. All the pictures were obtained at ×20 magnification.

(Table I) the penetration was only 6–9 µm or 3% deeper for SF than NBC. NBC being a poor candidate for iontophoresis (log P=4.99; MW=353.85 Da) and present at only 28 mM in the donor was expected to have a low transport number due to competition with the sodium ions (50 mM) in the donor. SF being more hydrophilic (MW=376.28 Da, log$P$=−0.67) and present as a single ion in the donor was, *a priori*, considered a much better candidate for iontophoretic

delivery. However, the SF donor solution had a pH ~ 8 to promote the marker ionization state and this could have provided the nail with a negative charge (31–34), thus SF delivery took place through a cation-selective nail. On the other hand, the NBC donor solution had a pH ~ 3, suggesting a positively charged nail which would be anion-selective. The pH dependence of the nail perm-selectivity and its impact on the iontophoretic transport of small inorganic cations and charged and unionized molecules has been demonstrated (30,31). Finally, the accumulation of chloride ions released at the cathode could have a deleterious effect on the transport of SF. For example, Sylvestre *et al.* (35) found the effect of chloride accumulation during transdermal iontophoresis to be dependent on the initial molar concentration of dexamethasone phosphate (log P=−0.30; MW=516.4 Da).

The maximum penetration (%T) measured in experiments exposing the dorsal layer to the donor solution was 11.2% of the nail. Thus, according to thickness ratio 3:5:2 (dorsal:intermediate:ventral) reported by Kobayashi (16), none of the markers penetrated the nail plate deeper than the dorsal layer (30%). Surprisingly, no differences in the penetration depth measured for SF were found when the dorsal layer was filed, in apparent disagreement with previous data reporting the dorsal layer as the main barrier to nail permeation (16). In previous work, the flux of 5-fluorouracil (130 Da, log$P$=−0.65) was higher across dorsal-filed nails than through full-thickness nails (16). However, direct comparison is not possible as the 5-FU data concerns the steady-state passive flux of a smaller permeant during longer (7 days) experiments. On the other hand, our results would agree with the model proposed by Nogueiras-Nieto *et al.* (20) for the nail plate microstructure that is, a more porous external layer which would be more easily penetrated by compounds and an inner less porous central layer.

Finally, some images were taken at objective ×20 to investigate the possible pathways of penetration for the two markers (Fig. 6). Interestingly, little differences were observed between passive and iontophoretic images obtained for NBC experiments and between the two markers iontophoretic experiments. In all cases, SF and NBC fluorescence was well distributed, suggesting an important contribution of the transcellular pathway. The intercellular pathway seemed darker in some of the images, suggesting a lesser role for this route. The surface of the ventral layer was slightly rougher and pitted compared to the dorsal layer a difference already reported using scanning electron microscopy (36,37) and atomic force microscopy (38). The more irregular surface of the intermediate layer is probably an artefact caused by the filing process. SF images presented small dark spots which were not present on NBC images (Fig. 6). Possibly, NBC was able to colour the complete cell including remnants of the nuclei (39); the darker intracellular areas not coloured by SF could represent the remnant of the disintegrated nuclei which have been already visualized (40). Further work is necessary to confirm these observations and to establish the contribution of each pathway to molecular permeation across the nail unequivocally.

CONCLUSIONS

A method to estimate the depth of penetration into human nail plate via confocal microscopy was developed; the value of three depth parameters was compared and the inter- and intra- nail variability associated to the measurements was assessed. Despite their different physicochemical properties, NBC and SF presented relatively similar depth of penetration under passive and iontophoretic conditions. Iontophoresis delivered the two markers slightly deeper into the nail than passive diffusion, but the level of enhancement was very moderate and independent of the intensity of current applied. SF passive and iontophoretic delivery into the dorsal, ventral or intermediate layer of the nail was very similar. Finally, the transcellular pathway of penetration into the nail plate was predominant for both markers and delivery methods.

ACKNOWLEDGMENTS AND DISCLOSURES

The authors gratefully acknowledge A. Rogers for his technical help on the LSCM. Dr J. Dutet thanks the University of Bath for her studentship.

REFERENCES

1. Murdan S. Enhancing the nail permeability of topically applied drugs. Exp Opin Drug Del. 2008;5(11):1267–82.
2. Green DM, Brain KR, Walters KA. Nail delivery. In: Rathbone MJ, Hadgraft J, Roberts MS, Lane ME, editors. Modified-release drug delivery technology, Vol 2. 2nd ed. New York: Informa Healthcare; 2008. p. 383–93.
3. Elkeeb R, AliKhan A, Elkeeb L, *et al.* Transungual drug delivery: current status. Int J Pharm. 2010;384(1–2):1–8.
4. Rotta I, Sanchez A, Gonçalves PR, Otuki MF, Correr CJ. Efficacy and safety of topical antifungals in the treatment of dermatomycosis: a systematic review. BJD. 2012;166(5):927–33.
5. Elewski B, Tavakkol A. Safety and tolerability of oral antifungal agents in the treatment of fungal nail disease: a proven reality. Ther Clin Risk Manag. 2005;1(4):199–306.
6. Mackay-Wiggan A, Elewski BE, Scher RK. The diagnosis and treatment of nail disorders: systemic antifungal therapy. Dermatol Ther. 2002;15(2):78–88.
7. Venkatakrishnan K, von Moltke LL, Greenblatt DJ. Effects of the antifungal agents on oxidative drug metabolism: clinical relevance. Clin Pharmacokinet. 2000;38(2):111–80.
8. Crawford F, Hollis S. Topical treatments for fungal infecrtions of the skin and nails of the foot (Review). Cochrane Libr. 2007;3:1–124.

9. Delgado-Charro MB. Iontophoretic drug delivery across the nail. Exp Opin Drug Del. 2012;9(1):91–103.
10. Amichai B, Nitzan B, Mosckovitz R, Shemer R. Iontophoretic delivery of terbinafine in onychomycosis: a preliminary study. Br J Dermatol. 2010;162(1):46–50.
11. Dutet J, Delgado-Charro MB. *In vivo* transungual iontophoresis: effect of DC current application on ionic transport and on transonychial water loss. J Control Release. 2009;140(2):117–25.
12. Turner NG, Guy RH. Visualization and quantitation of iontophoretic pathways using confocal microscopy. J Invest Dermatol. 1998;3(2):136–42.
13. Bath BD, Scott ER, Phipps JB, White HS. Scanning electrochemical microscopy of iontophoretic transport in hairless mouse skin. Analysis of the relative contributions of diffusion, migration, and electroosmosis to transport in hair follicles. J Pharm Sci. 2000;89 (12):1537–49.
14. De Berker DAR, Andre J, Baran R. Nail biology and nail science. Int J Cosmet Sci. 2007;29(4):241–75.
15. De Berker D, Mawhinney B, Svilan L. Quantification of regional matrix nail production. 1996; 134(6): 1083–1086
16. Kobayashi Y, Miyamoto M, Sugibayashi K, Morimoto Y. Drug permeation through the three layers of the human nail plate. J Pharm Pharmacol. 1999;51(3):271–8.
17. Parent D, Achten G, Stouffs-Vanhhof F. Ultrastructure of the normal human nail. Am J Dermatopathol. 1985;7(6):529–35.
18. Hashimoto K. Ultrastructure of the human toenail. Cell migration, keratinization and formation of the intercellular cemenr. Arch Derm Forsch. 1971;240(1):1–22.
19. Jarrett A. The histochemistry of the human nail. Arch Dermatol. 1966;94(5):652–757.
20. Nogueiras-Nieto L, Gómez-Amoza JL, Delgado-Charro MB, Otero-Espinar FJ. Hydration and n-acetyl-L-cysteine alter the microstructure of human nail and bovine hoof: Implications for drug delivery. J Control Release. 2011;156(3):337–44.
21. Alvarez-Román R, Naik A, Kalia YN, Fessi H, Guy RH. Visualization of skin penetration using confocal laser scanning microscopy. Eur J Pharm Biopharm. 2004;58(2):301–16.
22. Kaufman SC, Beuerman RW, Greer DL. Confocal microscopy: a new tool for the study of the nail unit. J Am Acad Dermatol. 1995;32(4):668–70.
23. Hongsharu W, Dwyer P, Gonzales P, Anderson RR. Confirmation of onychomycosis by *in vivo* confocal microscopy. J Am Acad Dermatol. 2000;42(2 part 1):214–6.
24. Sattler E, Kaestle R, Rothmund G, Welzel J. Confocal laser scanning microscopy, optical coherence and transonychial water loss for *in vivo* investigation of nails. BJD. 2012;166(4):740–6.
25. Nair AB, Vaka SRK, Sammeta SM, Kim HD, Friden PM, Chakraborty B, Murthy SN. Trans-ungual iontophoretic delivery of terbinafine. J Pharm Sci. 2009;98(5):1788–96.
26. Green PG, Hinz RS, Cullander C, Yamane G, Guy RH. Iontophoretic delivery of amino acids and amino acids derivatives across the skin *in vitro*. Pharm Res. 1991;8(9):1113–20.
27. Hao J, Smith KA, Li SK. Time-dependent electrical properties of human nail upon hydration *in vivo*. J Pharm Sci. 2010;99(1):107–18.
28. Walters KA, Flynn GL, Marvel JR. Physicocehmical characterization of the human nail: permeation patter for water and the homologous alcohols and differences with respect to the stratum corneum. J Pharm Pharmacol. 1997;35(1):28–33.
29. Mertin D, Lippold BC. *In-vitro* permeability of the human nail and of a keratin membrane from bovine hooves: Influence of the partition coefficient octanol/water and the water solubility of drugs on their permeability and maximum flux. J Pharm Pharmacol. 1997;49(1):30–4.
30. Kobayashi Y, Komatsu T, Sumi M, Numajiri S, Miyamoto M, Kobayashi D, Sugibayashi K, Morimoto Y. *In vitro* permeation of several drugs through the human nail plate: relationship between physicochemical properties and nail permeability of drugs. J Pharm Pharmacol. 2004;21(4):471–7.
31. Murthy SN, Waddell DC, Shivakumar HN, Balaji A, Bowers CP. Iontophoretic permselective property of human nail. J Dermatol Sci. 2007;46(2):150–2.
32. Murthy SN, Wiskirchen DE, Bowers CP. Iontophoretic drug delivery across human nail. J Pharm Sci. 2007;96(2):305–11.
33. Dutet J, Delgado-Charro MB. Transungual iontophoresis of lithium and sodium: effect of pH and co-ion competition on cationic transport numbers. J Control Release. 2010;144 (2):168–74.
34. Smith KA, Hao J, Li SK. Influence of pH on transungual passive and iontophoretic transport. J Pharm Sci. 2010;99(4):1955–67.
35. Sylvestre JP, Díaz-Marín C, Delgado-Charro MB, Guy RH. Iontophoresis of dexamethasone phosphate: competition with chloride ions. J Control Release. 2008;131(1):41–6.
36. Forslind B, Thyresson N. On the structure of the normal nail. A scanning electron microscope study. Arch Derm Forsch. 1975;251 (3):199–204.
37. Murdan S. Drug delivery to the nail following topical application. Int J Pharm. 2002;236(1):1–26.
38. Repka MA, O'Haver J, See CH, Gutta K, Munjal M. Nail morphology studies as assessments for onychomycosis reatment modalities. Int J Pharm. 2002;245(1–2):25–36.
39. Huang CZ, Li YF, Zhang DJ, Ao XP. Spectrophotometric study on the supramolecular interactions of nile blue sulphate with nucleic acids. Talanta. 1999;49(3):495–503.
40. de Berker D, Forslind B. The structure and properties of nails and perinugual tissues. In: Forslind B, Lindberg M, editors. Skin, hair and nails. Structure and function. New York: Marcel Dekker, Inc; 2004. p. 409–64.